Supplementary Materials

Imaging mass spectrometry of intraspecies metabolic exchange revealed the cannibalistic factors of *Bacillus subtilis*

Wei-Ting Liu,[a,1] Yu-Liang Yang,[b,1] Yuquan Xu,[b,1] Anne Lamsa,[c] Nina M Haste,[b,d] Jane Y. Yang,[a] Julio Ng,[e] David Gonzalez,[a] Craig D. Ellermeier,[f] Paul D. Straight,[g] Pavel A. Pevzner,[e,h] Joe Pogliano,[c] Victor Nizet,[b,d,i], Kit Pogliano,[c] Pieter C. Dorrestein,[a,b,d,2]

[a]*Departments of Pharmacology, Department of Chemistry and Biochemistry, University of California, San Diego, La Jolla, CA 92093.*
[b]*Skaggs School of Pharmacy and Pharmaceutical Sciences, University of California, San Diego, La Jolla, CA 92093.*
[c]*Division of Biological Sciences, University of California, San Diego, La Jolla, CA 92093.*
[d]*Center for Marine Biotechnology and Biomedicine, University of California, San Diego, La Jolla, CA 92093.*
[e]*Department of Computer Science, University of California San Diego, La Jolla, CA 92093.*
[f]*Department of Microbiology, University of Iowa, Iowa, 52242.*
[g]*Department of Biochemistry and Biophysics, Texas A&M University, College Station, TX 77843.*
[h]*University of California San Diego NCRR Center for Computational Mass Spectrometry, La Jolla, CA 92093.*
[i]*Department of Pediatrics, University of California San Diego, La Jolla, CA 92093.*

[1]The authors contributed equally to this work.
[2]Corresponding author
To whom correspondence should be directed, E-mail: pdorrest@ucsd.edu. Mailing address: Skaggs School of Pharmacy and Pharmaceutical Sciences, Biomedical Science Building (BSB), Room 4090 9500 Gilman Drive, La Jolla, CA 92093-0636. Phone: +1(858)534-6607. Fax: +1(858)822-0041.

A. Supporting text

Structural elucidation of SDP and SKF

The purified SDP was subjected to high resolution Fourier transform ion cyclotron resonance mass spectrometry (FT-ICR MS) to obtain a monoisotopic mass *m/z* 4311.209 $[M+H]^+$ (Fig. S3), and this mass matched Cys^{141}-Ser^{182} of SdpC-2.016 Da, indicating the likely presence of a disulfide crosslink. The fragmentation by collision-induced dissociation (CID) and FT-ICR MS analysis confirmed the sequence with a disulfide crosslink localized to residues Cys^{141} and Cys^{147} (Fig. 2, Fig. S5, Table S4). The N-terminal boundary of SDP is in agreement with the N-terminal Edman amino acid sequencing previously performed on SDP (1).

Purified SKF was also analyzed by high-resolution mass spectrometry and found to have a mass of 2781.302 Da (Fig. S3). This mass could not be readily matched to the C- or N-terminal portions of the 55 amino acid protein precursor SkfA (1). When purified SKF was subjected to high-resolution tandem mass spectrometry, the sequence tag WASKSI was obtained (Fig. S8*A*, Fig. S9). To define the number of amino acids that were involved in the mature SKF metabolite, a ^{15}N feeding experiment was performed. The feeding experiment with 98% pure [^{15}N]ammonium chloride resulted in a 36 Da increase in mass, indicating that SKF contained 36 nitrogen atoms which matched to the number of nitrogens in the last 26 amino acids of the SkfA sequence, CMGCWASKSIAMTRVCALPHPAMRAI (Fig. S8*B*). The calculated mass of this peptide is 2803.340, and therefore, the mature form of SkfA is 22.038 Da less than that expected from the intact peptide sequence. The absence of observable *y* ions provided an indication that SKF may be cyclic (2). We postulated that SKF was cyclic accounting for 18.011 of the 22.038 Da mass differences. The remaining 4.027 Da difference between the parent SkfA peptide and the cyclized precursor could be explained by two crosslinks, possibly a disulfide and a thioether.

To confirm that SKF was indeed cyclic, all thiols were replaced with a proton using a reductive dethiolation reaction composed of $NiCl_2$ and $NaBH_4$ (Fig. S10) (3). Subjecting SKF to this reaction resulted in an ion with a mass of 2551.444 Da. Tandem mass spectrometry by collision induced dissociation (CID) confirmed the sequence to the 26 amino acids on the C-terminal end of SkfA as well as a cyclic head-to-tail linkage between isoleucine and cysteine. The calculated mass of this molecule is 2551.450. To define the connection of the thioether linkage, the reductive dethiolation was repeated but with deuterated solvents and $NiCl_2/NaBD_4$ and resulted in a species with mass of 2558.491, 7.041 Da larger compared to the product resulted from $NiCl_2/NaBH_4$ reaction, suggesting 7 thiol connections. Six deuteriums were introduced from the replacement of three methionine and three cysteine side chains with deuterons while the remaining deuterium was introduced at the site of the thioether linkage (Fig. S11*A*). Therefore, it became possible to map out the position of the thioether linkage by locating this extra deuterium that gave rise to the 1 Da mass shift. To map the thioether linkage, multiple stages of tandem mass spectrometry were obtained on the deuterated dethiolated

SKF. To find the position of the additional deuterium, a mass list with manually deconvoluted fragment ions was analyzed by an algorithm NRP-comparative dereplication (4) against the theoretical structure of SKF with a deuterium labeled on each desulfurized position (Fig. S11*A*). NRP-dereplication matched the MS fragments with the structure and Met^{12} had the lowest score indicated the strongest correlation of the 1 Da increase between the observed ions in the tandem mass spectrometry experiment when compared to the theoretically predicted ions of the deuterated dethiolated SKF template (Fig. S8*C* and Fig. S11*B*). Guided by the NPR-dereplication result, manual annotation was performed, again verifying the extra deuterium on Met^{12} (Fig. S11*C* and Table S5, S6).

The position of the disulfide bond was determined by reduction, iodoacetamide alkylation and tandem mass spectrometry. Reduction and alkylation of SKF resulted in a mass increase of 116.061 Da, in agreement with two free thiols (Fig. S10). Via tandem mass spectrometry, the alkylated residues were found to be Cys^1 and Cys^{16}, positioning the disulfide between these two cysteines. Even though the tandem mass spectrometry of the desulfurized SKF indicated that the thioether linkage is connected to the methionine, it did not provide regiochemical information to which carbon of Met^{12} that Cys^4 was connected. To determine the regiospecificity of the tetrahedral linkage, we resorted to nuclear magnetic resonance (NMR) spectroscopy (Figs. S12 and Table S7). To determine the relevant proton signals, the NMR signal that corresponded to the methionine involved in the thioether cross-link needed to be identified. To find the modified methionine with an absent proton, a ^1H-^1H total correlation spectroscopy (TOCSY) was obtained first. From the TOCSY, one set of methionine correlations lacking an α-proton was observed, and suggested that the linkage of Cys^4 to Met^{12} is via the α-carbon of the latter residue (Fig. S12*B* and C). An α-connection would result in a ^{13}C-chemical shift at this α-carbon of about 70 ppm while a β-connection would result in ^{13}C-chemical shift of 40-50 ppm (3). The ^{13}C-chemical shift information was obtained indirectly by heteronuclear multiple bond correlation (HMBC) (Fig. S8*D* and *E*, Fig. S12*D*), because of the small quantities of pure SKF available. The same methionine that was missing the proton in the TOCSY was scrutinized in the HMBC spectrum. In the HMBC, in agreement with the findings by TOCSY, there was no evidence of an α-proton in Met^{12}; however, the β-proton possessed long range correlations between the β-protons and two quaternary carbons, located at δ 67.9 and 180.7 (Fig. S8*D* and *E*), and thus consistent with a thioether bridge connecting to the α-carbon of Met^{12}. A post-translational modification of a cysteine to the α-carbon of methionine has not been previously reported (5).

The functional annotation of the *skf* biosynthetic operon.

Based on the structure of SKF, it is now possible to propose the role of each gene on the *skf* operon involved in SKF biosynthesis. The *skf* operon was previously predicted to contain a stop codon due to sequencing errors in the original genome that resulted in an incorrect open reading frame assignment for *skfC*

and *skfD* (1). Thus, *skfC* and *skfD* are in fact a single open reading frame, and therefore we have omitted the designation *skfD*. Therefore the *skf* operon has seven genes, *skfABCEFGH* (Fig. S13). SkfA is a prepropeptide that is post-translationally modified to the mature SKF (1). SkfB belongs to the radical SAM superfamily that includes genes such as *albA*, *lipA*, *bioB*, which are involved in the biosynthesis of C-S linkages in subtilosin, lipoic acid, and biotin, respectively (Fig. S14*A*) (3, 6-8). We propose that SkfB is responsible for the C-S linkage of Cys^4 to the α-carbon of Met^{12} similar to the proposed reaction catalyzed by AlbA on the subtilosin pathway (3, 9). SkfC belongs to the CaaX family of proteases (Fig. S14*B*) which, in eukaryotes, are responsible for the proteolysis of C-terminal prenylated cysteines (10). Since this is the only protease candidate on the *skf* gene cluster, we propose it is involved in the cyclization reaction, which would represent a new function for a CaaX family member of proteins. SkfE is homologous to the cytoplasmic ATPase domain of ABC transporters, while SkfF is a polytopic membrane protein; both are predicted to be involved in the export and immunity of SKF (1). SkfG showed homology to several HEAT-repeat containing proteins, although the role of SkfG remains unclear. SkfH is a thioredoxin-oxidoreductase like protein and may be involved in the generation of the disulfide bond analogous to the proposed function of the oxidoreductase on the sublancin 168 biosynthetic pathway (Fig. S14*C*) (11).

B. Supplementary Methods

Strains used in this study

Bacillus	Genotype	Background	Source – Ref.
3610	Prototroph		S. Branda – 12
PY79	Prototrophic derivative of *B. subtilis* 168		K. Pogliano – 13
KP648	Δ*spo0A::erm*	PY79	K. Pogliano – 14,15
ALB1035	Δ*spo0A::erm*	3610	This study
EG208	$P_{spac\text{-}hy}$-*skfABCDEFGH(kan)*	PY79	R. Losick – 1
EG165	Δ*skfA::spc*	PY79	R. Losick – 1
EH273	*sdpABC*::*kan*	PY79	R. Losick – 16
ALB1046	Δ*skf::cat*	PY79	This study
ALB1085	$P_{spac\text{-}hy}$-*skfABCDEFGH(kan), ΔsdpABIC::tet*	PY79	This study
CDE1160	*amyE::*$P_{spac\text{-}hy}$-*sdpC(spec), sdpC::tet,* $P_{spac\text{-}hy}$-*sdpAB(cat)*	PY79	This study

Thin-layer agar MALDI-IMS

Sample preparation for thin-layer agar MALDI-IMS experiments was performed using a modified method adjusted from reference 17. 0.2-1 μL of bacterial overnight cultures grown in LB media were spotted on 100 O.D. x 25 mm Petri dishes (Fisherbrand) containing ISP2 solid agar. For testing individual cultures in isolation, strains were spotted at the center of Petri dishes; for the PY79 and Δ*spo0A* co-culturing experiment, both strains were spotted on the same plate with a distance between spots of 0.75 cm. The Petri dishes were sealed with parafilm and incubated for 2-4 days as indicated. After culturing, a rectangular section containing the colonies

was transferred to a MALDI target plate. It is critical to avoid any air bubbles because it will cause the agar to peel off during the IMS process. After taking a photograph, a 1:1 mixture of α-cyano-4-hydroxycinnamic acid and 2,5-dihydroxybenzoic acid was sprinkled on top of the culture using a 20 μm sieve method (17, 18), and was dried in a 37 ^{o}C oven for three hours. The detailed instrument parameters for collecting image data were described in reference 17. Briefly, the sample was subjected to Bruker microflex MALDI-TOF MS for imaging MS acquisition and the data was analyzed using the FlexImaging 2.0 software.

Purification of SKF and SDP

PY79 was cultured on approximately 1000 IPS2 agar plates and cultured at 28 ^{o}C for 2 days. The bacteria were scraped from agar plates and then re-suspended in milli-Q water. Equal amount of *n*-BuOH was used to extract SKF and SDP from aqueous layer. The crude *n*-BuOH extract was lyophilized, re-dissolved and then eluted via Sephadex LH-20 column using isopropanol/MeOH = 1:9. Each fraction was analyzed by MALDI MS and the fractions containing signals *m/z* 2782 or *m/z* 4312 were collected into two separate tubes. The two tubes that contained crude SKF or SDP, respectively, were purified subsequently by HPLC (C-18, 250 x 4.6 mm) running a gradient from 25% solvent A to 70% solvent A in 60 minutes with flow rate 1mL/min. Solvent A is isopropanol/MeCN = 7:3 containing 0.1% TFA; solvent B is 0.1% TFA (aq). SKF and SDP were eluted at 14, and 34.5 min, respectively (Fig. S3). Purified SKF and SDP were lyophilized and stored at -80ºC before using for bioassay and structural elucidation. The yield for SKF and SDP was ~ 0.5 μg each per plate.

SKF derivatization

Dethiolated SKF was prepared by dissolving 1 μg of SKF with 1.5 μg $NaBH_4$/$NaBD_4$ and 1.5 μg $NiCl_2$ in 6.25 μL of 60% MeOH/MeOD. This reaction was incubated at 50 ^{o}C, and an additional 1.5 μg of $NaBH_4$/$NaBD_4$ and $NiCl_2$ were added into the reaction 5 and 10 minutes after initiation of the reaction to ensure complete conversion of SKF into dethiolated SKF. The mixture was then centrifuged for 1 min at 14500 rpm to remove the insoluble particles and then purified by HPLC using an Agilent Eclipse XDB-C18 column running MeCN gradients or by C18 ZipTip (Millipore) following the manufacturer's protocol prior to MS analysis.

For disulfide bond reduction, 1 μg SKF was dissolved in 40 mM ammonium bicarbonate buffer, pH 8.0, containing 10% MeCN. TCEP was added to reach a final concentration of 20 mM and incubated at 85 ^{o}C for 1hr. To prevent the free thiols from reforming disulfide bond, iodoacetamide was used to cap the cysteine thio group. To accomplish this, 50 mM Tris buffer, pH 7.4 was added to TCEP treated SKF solution to a final concentration of 1 mM to bring up the pH to neutral (checked by pH paper). 5 μg of iodoacetamide powder was directly added into the reaction mixture and allowed to react at RT for 5 min followed by quenching with an

equal volume of 10% formic acid.

General MS procedure for the characterization of SKF

For the MS data acquisition, each compound was dissolved in spray solvent 50:50 MeOH/H_2O containing 1% formic acid, and underwent nanoelectrospray ionization on a biversa nanomate (Advion Biosystems, Ithaca, NY) using a back pressure of 0.3-0.5 p.s.i. and the spray voltage of 1.4 -1.5 kV. MS spectra were acquired on a 6.42 T Finnigan LTQ-FTICR MS or a Finnigan LTQ-MS (Thermo-Electron Corporation, San Jose, CA) running Tune Plus software version 1.0 and Xcalibur software version 1.4 SR1. The instrument was first autotuned on the *m/z* value of the ion to be fragmented. Then, the ions were isolated by the linear ion trap and fragmented by collision induced dissociation (CID) (isolation window: 3-10 *m/z*; collision energy: 30).

NMR measurement of SKF

400 µg SKF was dissolved in 40 µL of CD_3OD for NMR data acquisition. NMR spectra were recorded on Bruker Avance III 600 MHz NMR with 1.7 mm Micro-CryoProbe at 300 K, with standard pulse sequences provided by Bruker. 2D TOCSY spectra were recorded with mixing times of 90 ms. 2D ^{1}H-^{13}C HMBC spectra were recorded with ^{2}J or $^{3}J_{H\text{-}C}$ coupling constants at 7 Hz, 2D ^{1}H-^{13}C HSQC spectra were recorded with $^{1}J_{H\text{-}C}$ coupling constants at 145 Hz.

Effect of SKF and SDP on *B subtilis* cell growth curve

The effect of SKF and SDP on *B. subtilis* cell growth was performed using 96 well microtiter plates. A 2 mL overnight culture in LB media was centrifuged at 6000g for 10 minutes and supernatants discarded. The cell pellets were resuspended using 2 mL of ISP2 media. OD_{595} of the resuspended cells were measured (ELx808 Ultra Microplate Reader, Bio-TEK Instruments), and the final OD_{595} was adjusted to 0.03 with ISP2 media. 100 µL diluted culture with indicated working concentrations of SKF or SDP were aliquoted into each well. The plate was shaken at 37°C, 120 rpm. OD_{595} were measured and recorded at each time point. To evaluate the effect of SDP on an exponentially growing culture, SDP was added at 3 or 6 hours to a final concentration of 20 µg/mL, and the OD_{595} was measured at each time point**.**

Fluorescence microscopy

The effects of SDP on individual *B. subtilis* cells were investigated in 15 µL cultures prepared in the following manner. Cultures were grown in LB media to an OD_{600} of 0.3, centrifuged, resuspended in 1/10 the volume and 14.25 µL of concentrated cells were added to 1.7 mL microcentrifuge tubes. At t = 0, 0.75 µL of 10% DMSO or 400 µg/mL SDP (in 10% DMSO) was added to different aliquots of cells. The tubes were capped and incubated

at 37°C in a roller. Samples were collected for imaging every 30 minutes. 2 µL of cells were added to 0.5 µL of a stain mix containing 30 µg/mL FM 4-64, 2.5 µM Sytox Green and 1 µg/mL DAPI prepared in 1X T-base. Cells were immobilized with Poly-L-Lysine and imaged on an Applied Precision Spectris Microscope (19). Images were deconvoluted and the medial focal planes shown. Time-lapse imaging showing the formation of membrane tubules and projections was performed on these slides, collecting images of cell membranes every 3 seconds for 1 minute.

Quantification of the amount of cellular lysis was performed by determining the percent cells showing clearly discontinuous membranes and increased permeability to Sytox Green relative to the number of intact cells. This data showed that the 3610 strain, both with and without the Δ*spo0A* mutation (ALB1035) showed the most rapid onset of cell lysis (first evident at t = 60 minutes) and the highest frequency of lysis. The strains in PY79 background were affected more slowly and in a lower percent of cells. We did not score later time points in this manner, because the extensive cell lysis made it impossible to determine the percent cell lysis, since it was unclear how many cells produced the debris.

Spot assay

Lawns were created by mixing 50 µl exponentially growing cells (OD_{600} = 0.4-0.6) with 3.5 ml 0.35% LB agar and pouring the mixture onto LB plates. When indicated, IPTG was added to a final concentration of 1 mM. After the top agar solidified, 5 µl of exponentially growing cells or purified compounds were spotted on top of the lawn and allowed to dry. The plates were then incubated overnight at 30°C.

Screen of antibacterial activities against pathogens

The activities of SDP and SKF were tested in a microtiter based screen for growth inhibitory activity against a variety of Gram-positive and Gram–negative bacterial species. Then, the IC_{50} of these compounds was assessed against a smaller set of representative organisms. For this assessment, SDP was tested against three organisms whose growth it inhibited, methicillin-resistant *Staphylococcus aureus* (MRSA) sequence type 59 (ST59), *S. aureus* Newman, *Staphylococcus epidermidis* (ATCC35984), and two that were unaffected, *Klebsiella pneumoniae* (ATCC700603) and *Pseudomonas aeruginosa* (ATCC 10145). SKF had no effect in the microtiter assay for any species and the MIC assay was performed with *S. aureus* MRSA ST59, *K. pneumoniae* (ATCC700603 and ATCC 35657), *Burkholderia cepacia* (ATCC 17765) and *Escherichia coli* (ATCC 25922).

IC_{50} assays were performed by a microbroth dilution assay. The overnight culture of the tested strain was diluted 1:200 in cation-adjusted Mueller-Hinton broth (MHB, Hardy Diagnostics, Santa Maria, CA) and grown with shaking at 37°C to mid-logarithmic phase after which they were centrifuged and pellets were resuspended

in phosphate-buffered saline to an OD_{600} of 0.4 – 0.5. Prior to the addition of this pre-culture, 96-well polystyrene test plates (Costar® #3288, Corning, NY) containing duplicate samples of serially diluted test compounds, SDP or SKF, and appropriate antibiotic controls were prepared in CAMHB. Bacteria were added to the test plate to a final concentration of $5x10^5$ CFU/ml in a volume of 80 µl/well. The control antibiotics included vancomycin (Hospira, Lake Forest, IL, USA) for *Staphylococcal* strains, ciprofloxacin (Fluka, Sigma-Adlrich) for *Pseudomonas aeruginosa* and sulfamethoxazole, trimethoprim (SMX-TMP Sicor ™ Irvine, CA) for *K. pneumoniae* and *E. coli* strains. Following the addition of bacteria, test plates were incubated at 37°C in a shaking incubator for 20 - 22h. Finally the plates were assessed for bacterial growth by the presence of turbidity at OD_{600}. The absorbance at each tested concentration were normalized to the negative control (absence of test compound) to determine relative growth at a given concentration of SDP or SKF. The IC_{50} values of SDP were determined from this data.

C. Supplementary Figures

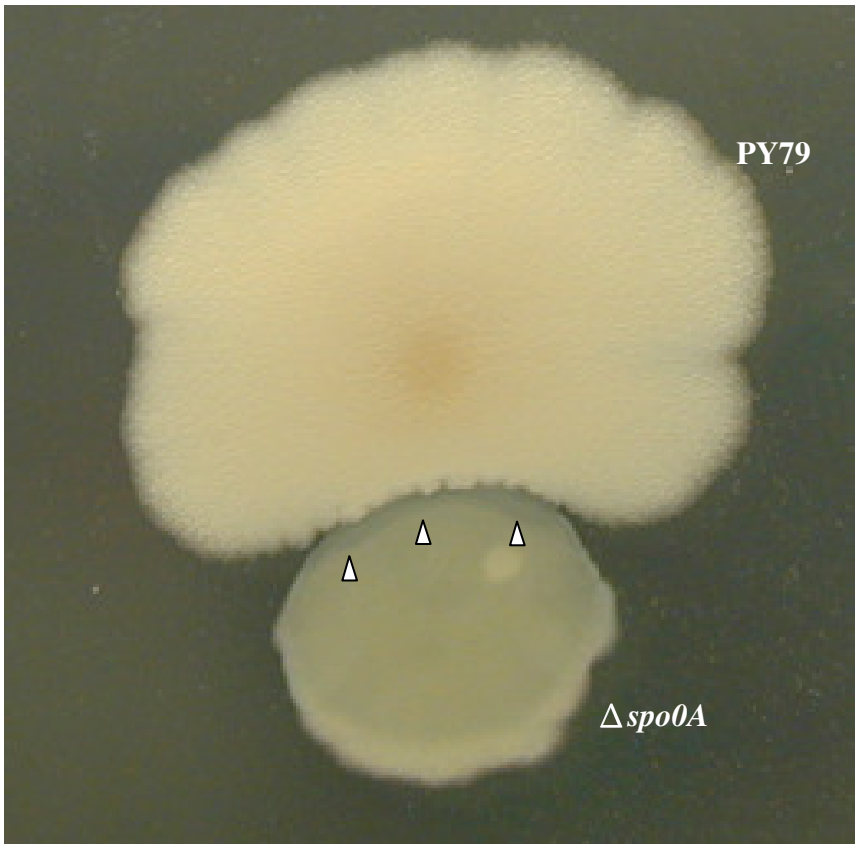

Supplementary Fig. 1. PY79 inhibits Δ*spo0A* (KP648) strain. The arrows (Δ) indicate the glassy region in the Δ*spo0A* colony.

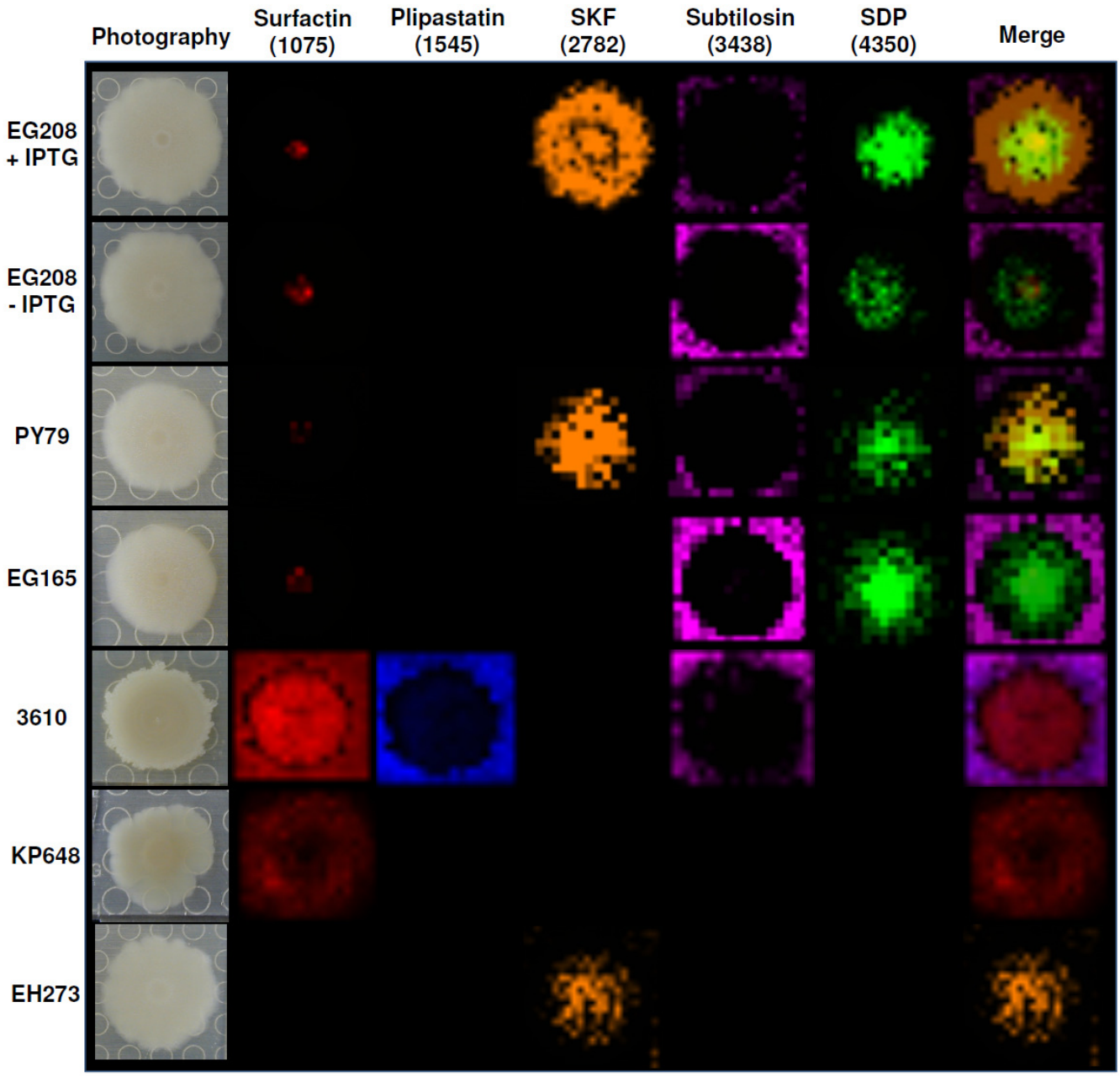

Supplementary Fig. 2. Metabolic profile of the strains used in this study. Strains were inoculated on an ISP2 agar plate and allowed to grow for 96 hours at room temperature and subjected to thin-layer agar IMS. The number labeled below each metabolite is the representative ion observed (*m/z*). *m/z* 1045, 1545, 3438 and 4350 are potassium adduct form $[M+K]^+$. For brief genotype description, 3610 is a wild type strain; PY79 is a laboratory domesticated wild type; EG208 contains the *skf* gene cluster under control of an IPTG inducible promoter; EG165, KP648, EH273 are *skfA, spo0A, sdpABC* deletion strains, respectively. All four mutants are constructed under PY79 background. The ion intensity was reflected by the intensity of colors. Each column of ions was displayed using same intensity scale optimized per each metabolite. The scale range in normalized relative ion intensity for each ion was specified in FlexImaging 2.0 (Bruker) as follows: surfactin 10%-100%; plipastatin 10-80%; SKF 30-60%; subtilosin 20-60%; SDP 1-30%.

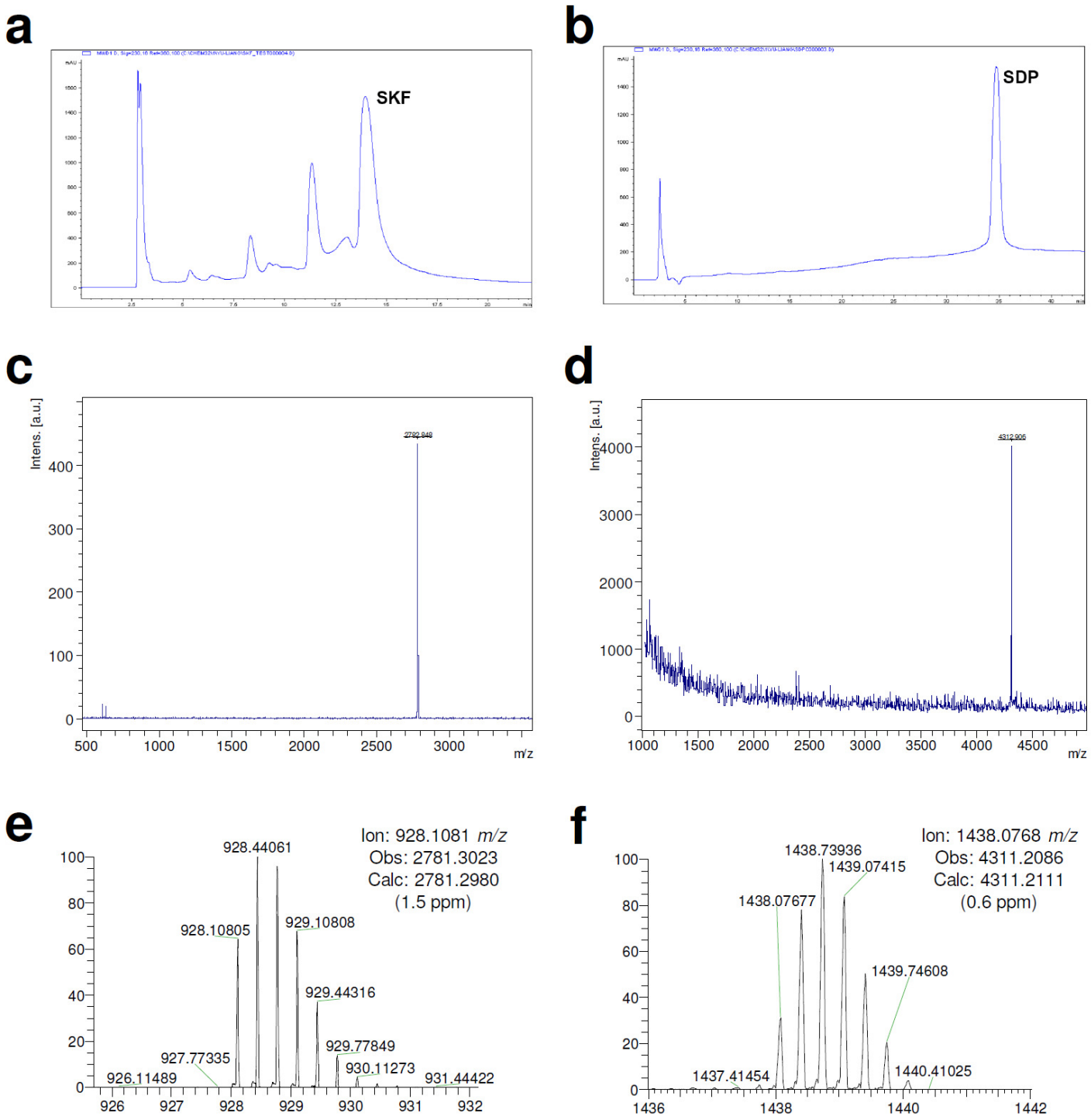

Supplementary Fig. 3. SKF and SDP purification. a, b) Crude SKF and SDP fractions obtained from an initial separations using Sephadex LH-20 column were further purified by HPLC (solvent system and gradients were specified in **Supplementary methods**). UV 230 nm was used to detect SKF and SDP. SKF and SDP were eluted at 14, and 34.5 min, respectively. **c**) MALDI-TOF MS spectrum of purified SKF. **d**) MALDI-TOF MS spectrum of purified SDP. **e**) FT-ICR MS spectrum of purified SKF. **f**) FT-ICR MS spectrum of purified SDP.

a

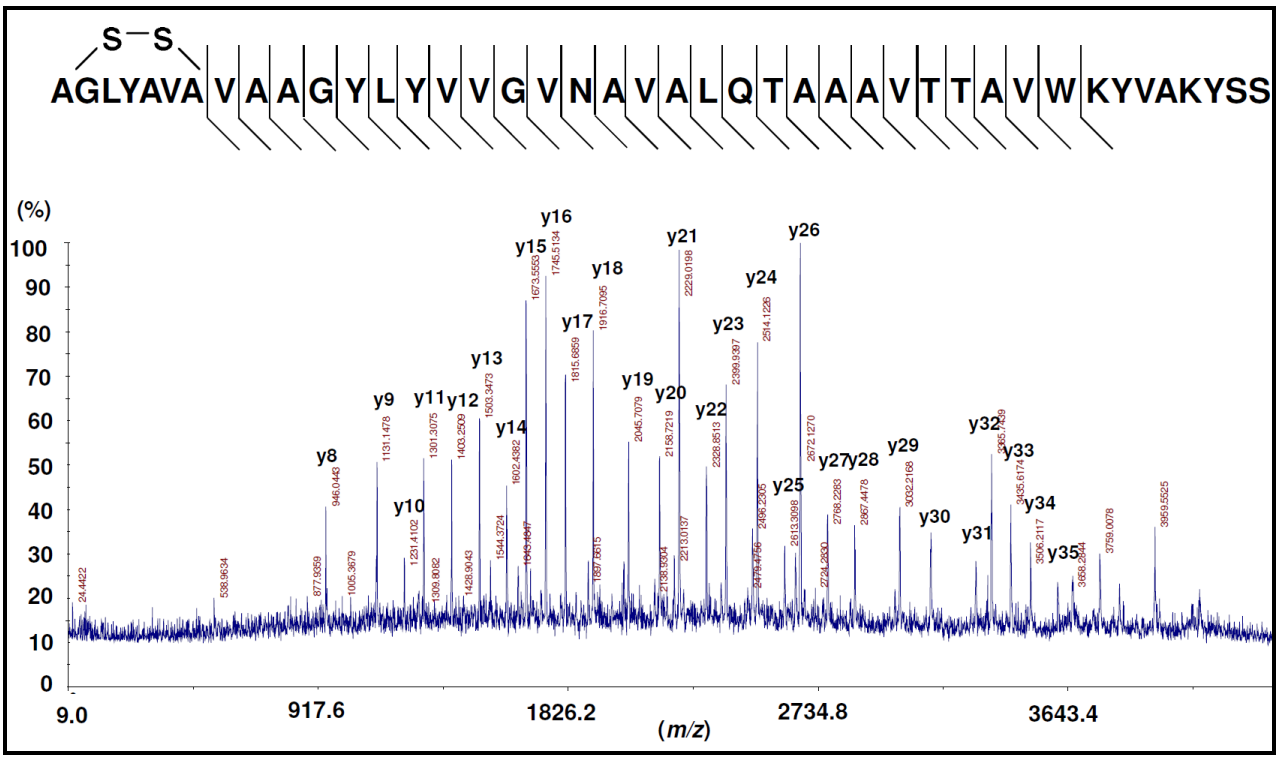

b

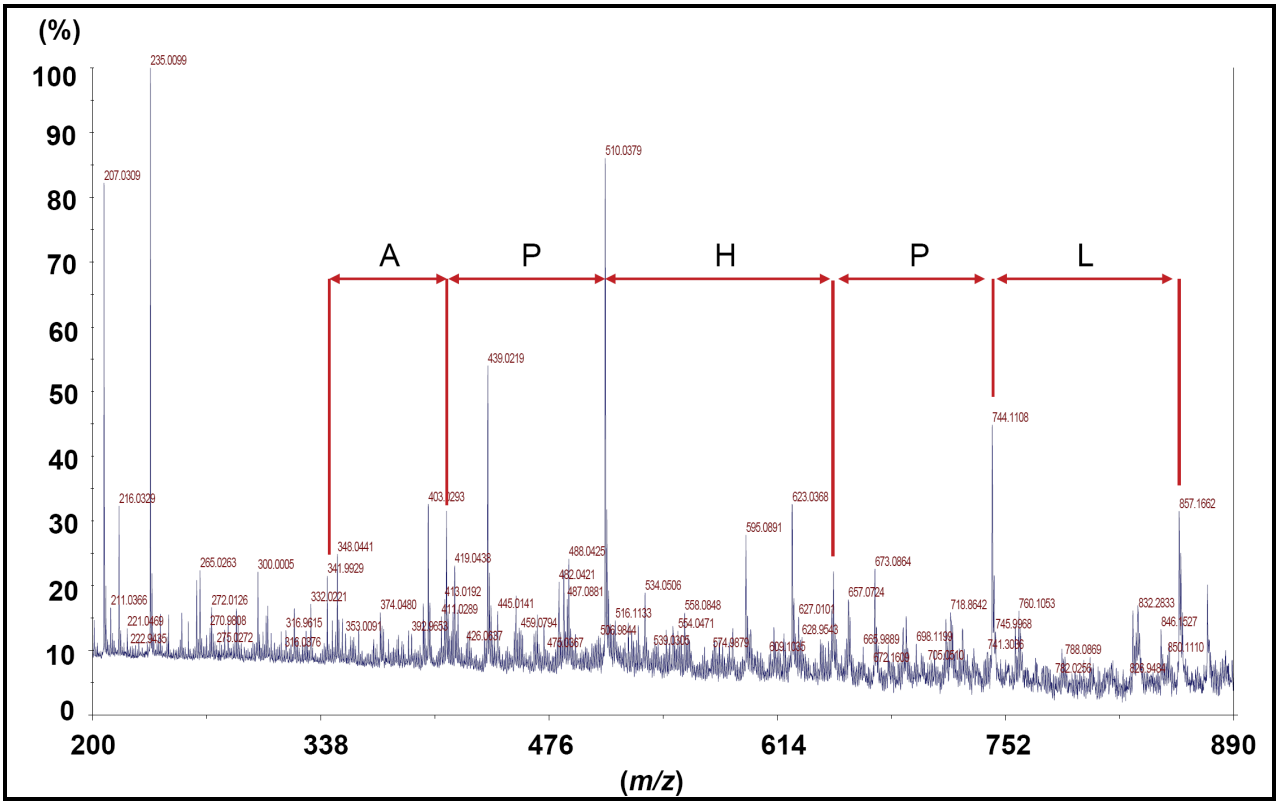

Supplementary Fig. 4. Intact cell MALDI TOF/TOF spectrum. a) Intact cell MALDI TOF/TOF spectrum of ion at *m/z* 4312. The corresponding ion table is showed in **Supplementary Table 1. b)** Intact cell MALDI TOF/TOF spectrum of ion at *m/z* 2782. The observed sequence tag that matched to SkfA is shown.

a)

```
atgaaaagtaaattacttaggctattgattgtttccatggtaacgatattggtttttca
ttagtaggactctctaaggagtcaagtacatctgctaaagaaaaccatacattttctgga
gaagattactttagaggacttttatttggacaaggggaagttggtaaattaatttcaaac
gatttggaccctaaactcgtaaaagaggcaaatagtacagaaggtaaaaagttagtaaat
gatgtagtcaaatttataaaaaaagatcaaccacaatatatggatgaattgaaacaatcg
attgacagcaaagaccctaaaaaactcattgaaaatatgaccaaagcagaccaacttatc
caaaaatatgctaagaaaaatgaaaacgtaaaatactcttctaataaagttactccatct
tgtgggctttatgccgtctgtgtagcagctggatatttatatgttgtgggcgttaacgca
gttgcattacaaacggctgccgcagtaacaactgcagtgtggaaatacgttgccaaatat
tcctcttcagcttctaataattctgatttagaagcggctgctgcaaaaaccctaaaattg
attcatcaataa
```

b)

```
        10         20         30         40         50         60
MKSKLLRLLI VSMVTILVFS LVGLSKESST SAKENHTFSG EDYFRGLLFG QGEVGKLISN
        70         80         90        100        110        120
DLDPKLVKEA NSTEGKKLVN DVVKFIKKDQ PQYMDELKQS IDSKDPKKLI ENMTKADQLI
       130        140        150        160        170        180
QKYAKKNENV KYSSNKVTPS CGLYAVCVAA GYLYVVGVNA VALQTAAAVT TAVWKYVAKY
       190        200
SSSASNNSDL EAAAAKTLKL IHQ
```

Supplementary Fig. 5. a) *sdpC* gene sequence. b) SdpC protein sequence. Mature SDP is highlighted in yellow. A disulfide bridge exists between C^{141} and C^{147}.

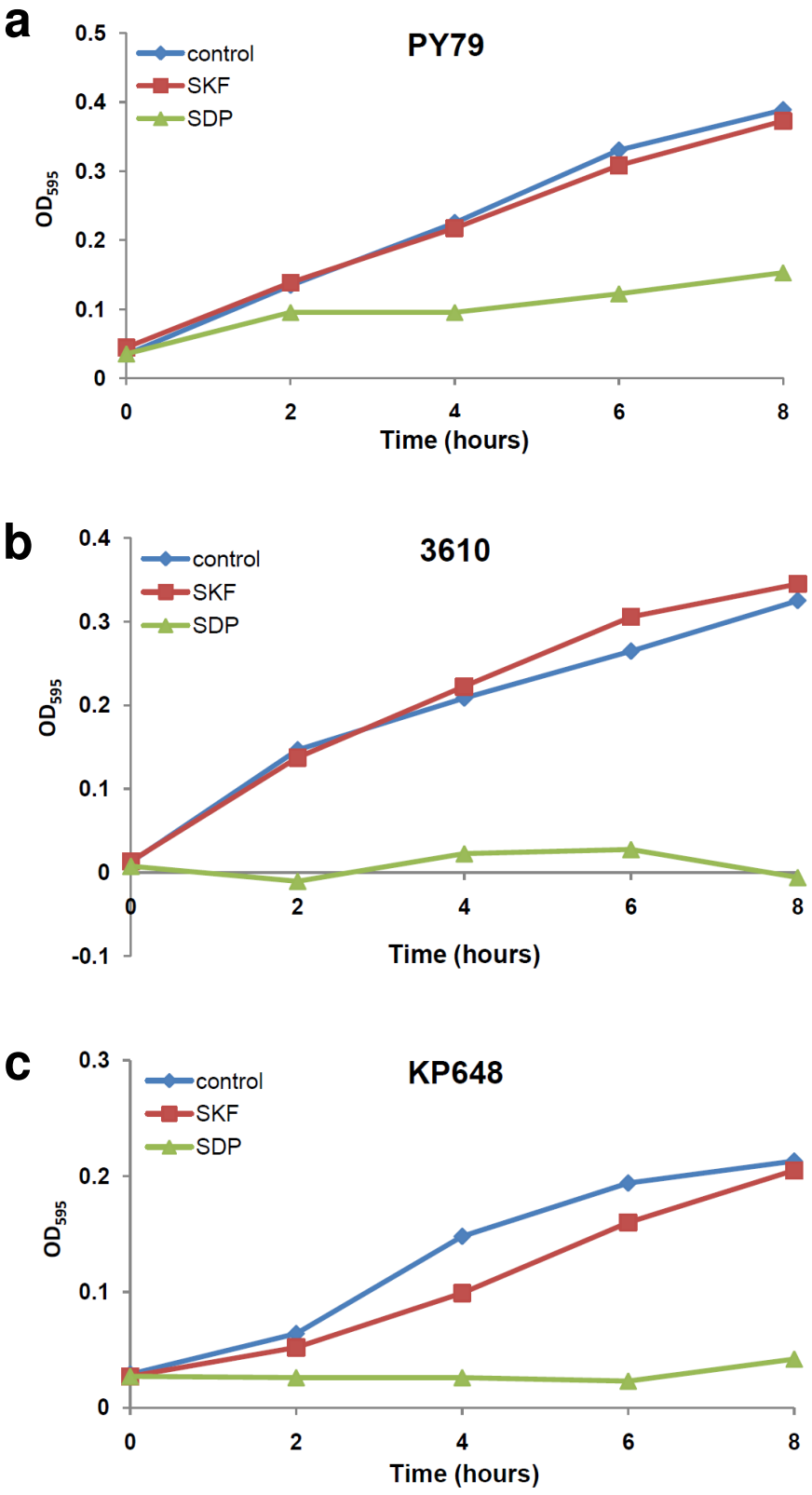

Supplementary Fig. 6. The effects of SDP and SKF on growth of *B. subtilis* strains in ISP2 media. The overnight culture was diluted into ISP2 media to OD_{595} 0.03, and SKF or SDP were added into 100 µL of diluted cultures to a final concentration of 20 µg/mL. The plate was shaken at 37 ^{o}C, 120 rpm. The OD_{595} was measured at each time point.

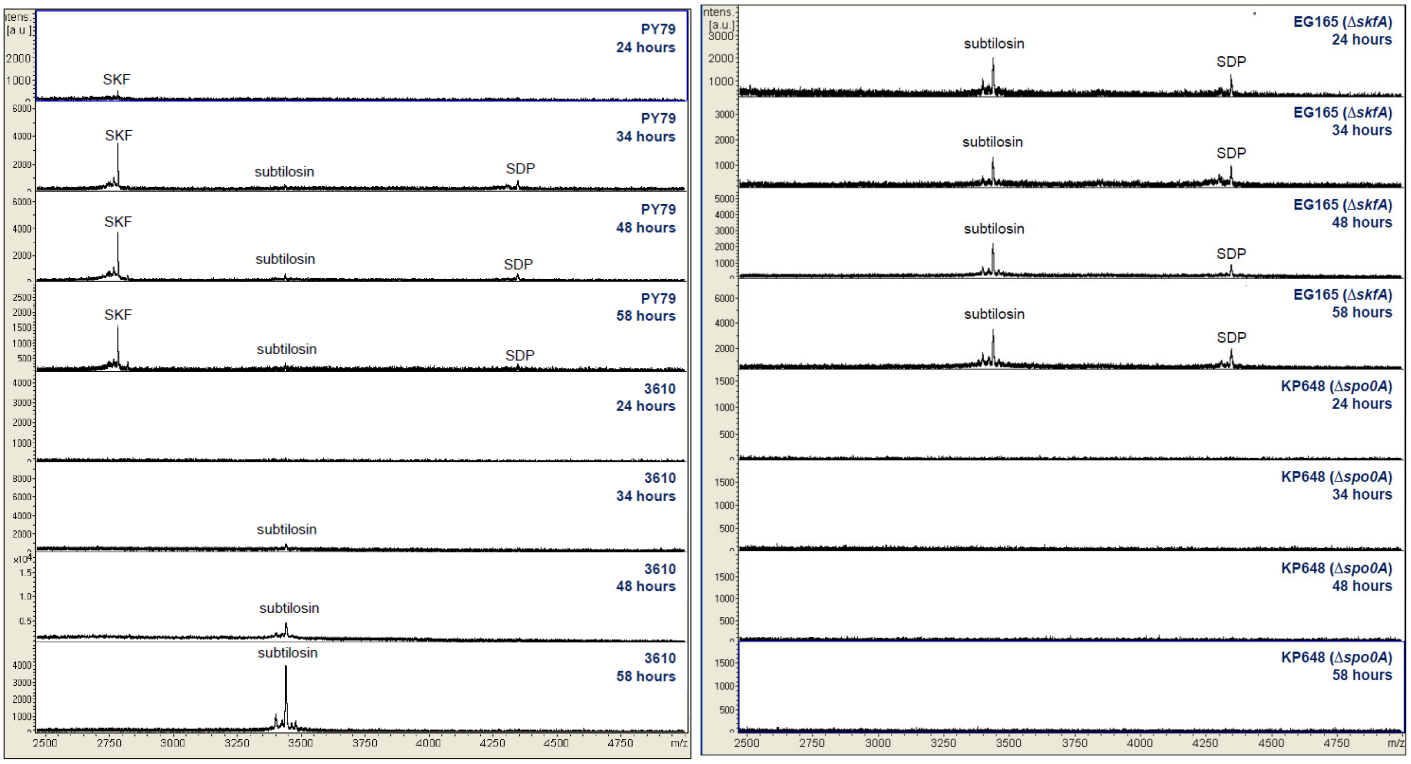

Supplementary Fig. 7. Time course of *B. subtilis* wildtype and mutant strains collected by intact cell MALDI-TOF MS (20, 21). Each strain was allowed to grow on ISP2 solid agar for 24, 34, 48 and 58 hours at 28 ºC. Each spectrum shown is an average of 200 single spectra. EG165 and KP648 are *skfA* or s*po0A* gene deletion strains, respectively. The metabolic outputs for 96 hours cultures are shown in **Supplementary Fig. 2**.

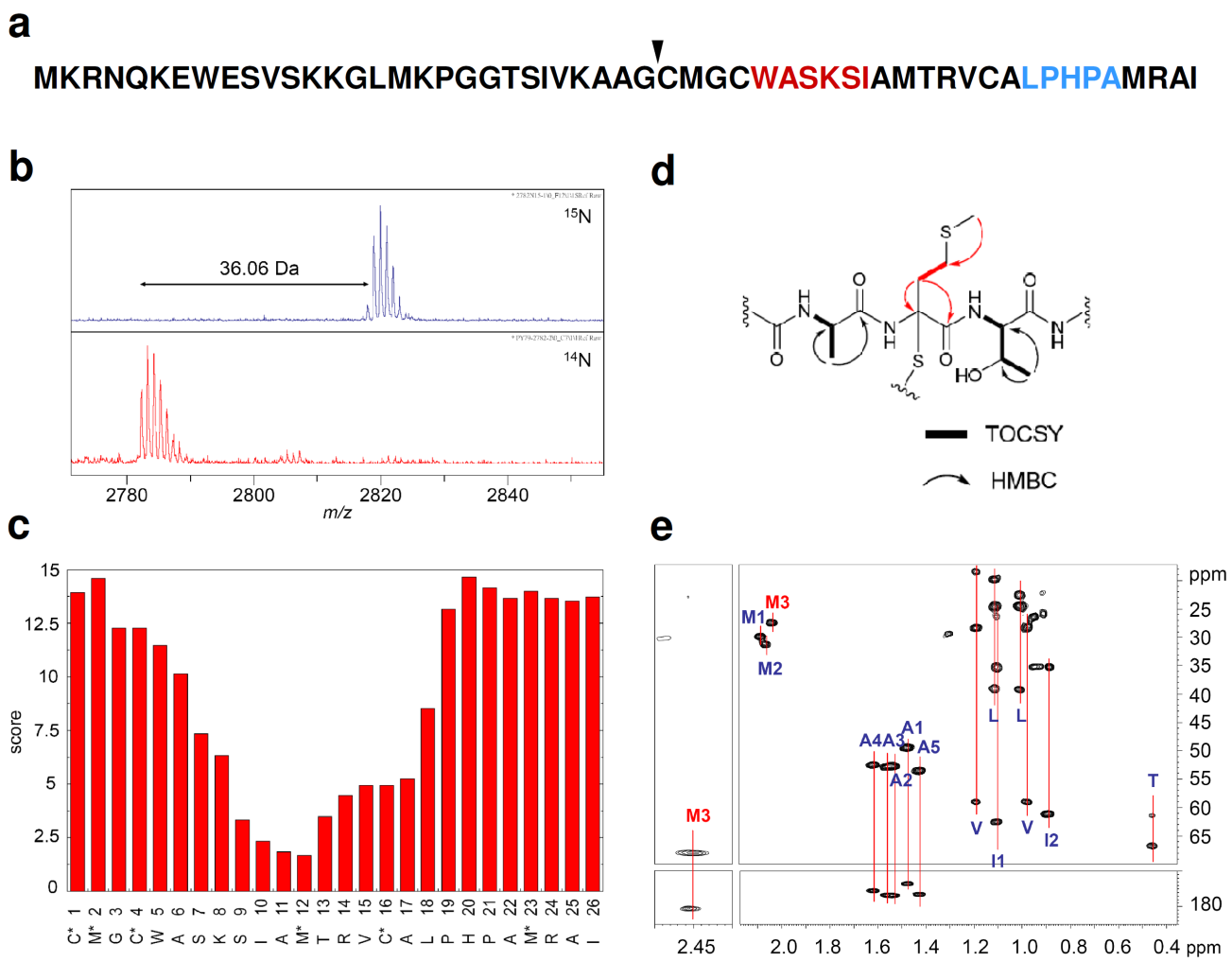

Supplementary Fig. 8. The structural characterization of SKF. (**a**) The SkfA sequence. ▼ indicates a protease cleavage site. The sequence tags observed by tandem mass spectrometry generated by FT-ICR MS/MS (red) and MALDI TOF/TOF (blue) are highlighted. (**b**) The MALDI-TOF analysis of SKF from cells grown in ^{15}N-media. (**c**) Comparative dereplication of deuterated-dethiolated SKF. (**d**) A schematic representation of the ^{1}H-^{13}C long range correlations and ^{1}H-^{1}H TOCSY correlations of the modified methionine and neighbor residues in SKF. (**e**) The ^{1}H-^{13}C HMBC spectrum of SKF showing the important ^{13}C-chemical shift supporting the α-connection to the methionine. The full TOCSY and HMBC spectra and tables of the observed chemical shifts are provided in the supporting information.

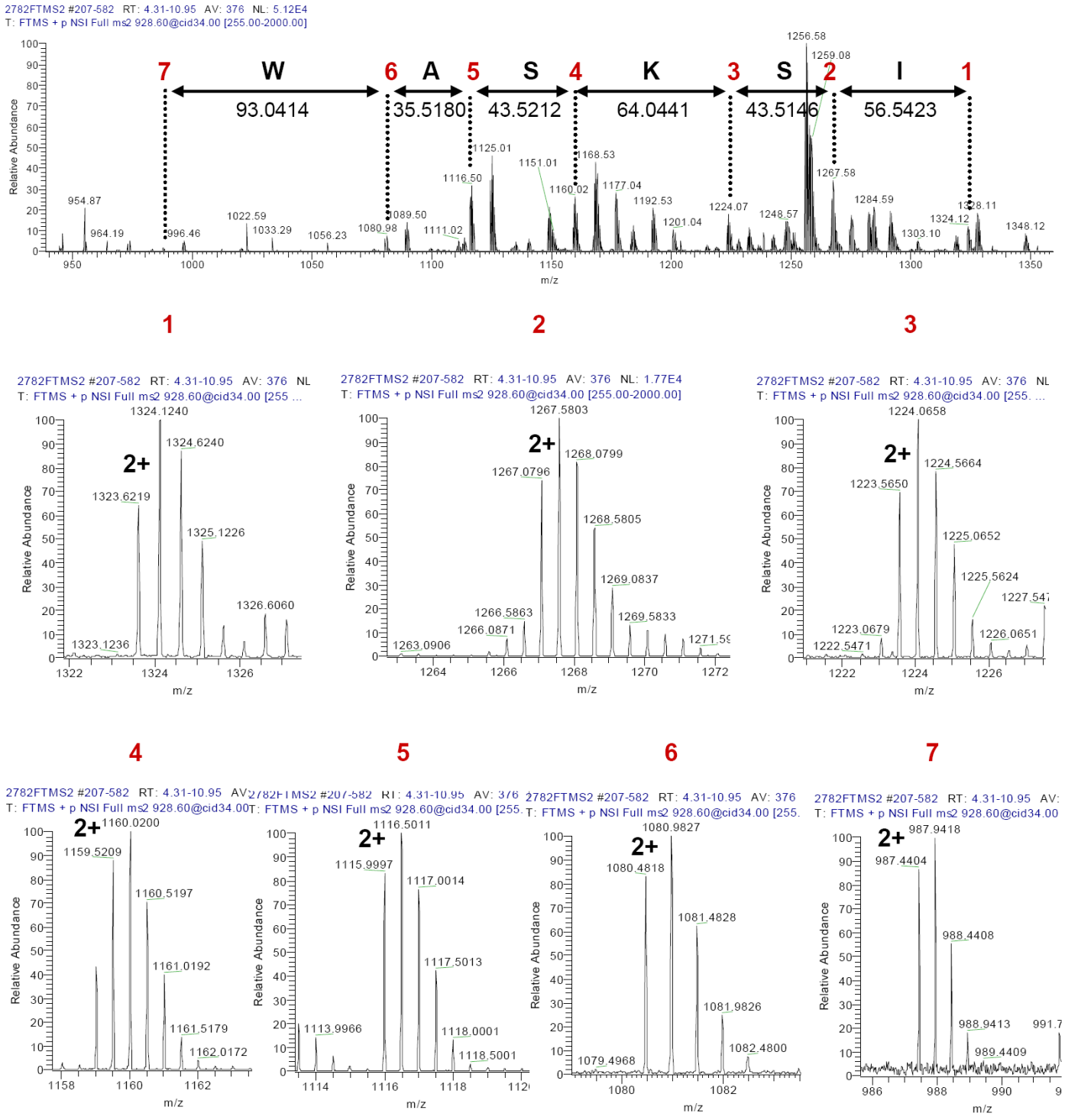

Supplementary Fig. 9. FT MS/MS spectrum of ion *m/z* 928.60 (2+ charge state). The observed mass difference and isotope profiles of each ion (2+ charge state) are shown.

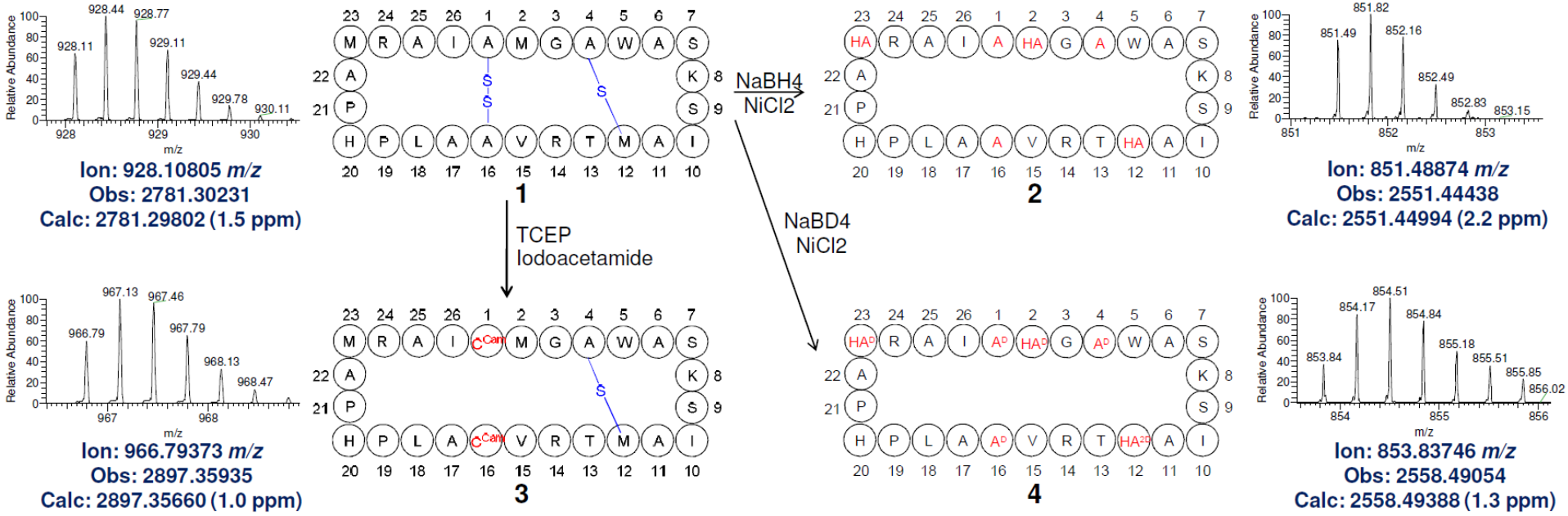

Supplementary Fig. 10. Chemical derivatization of SKF. TCEP reduction followed by iodoacetamide alkylation yielded a species with 116 Da addition (compound 2), corresponding to two carboxyamidomethylated cysteines (C^{Cam}) with the retaining of the thioether linkage. $NaBH_4$ and $NaBD_4$ reduction yielded dethiolated SKF derivatives with cysteine reduced to alanine, and methionine to homoalanine (HA) (compound 3,4). Deuteriums were labeled on the reductive cleavage positions under deuterated condition (compound 4). Zoom in MS1 spectrum of 3+ charge state species analyzed by FT-ICR MS as well as observed (Obs) and calculated (Calc) masses were showed beside each derivative.

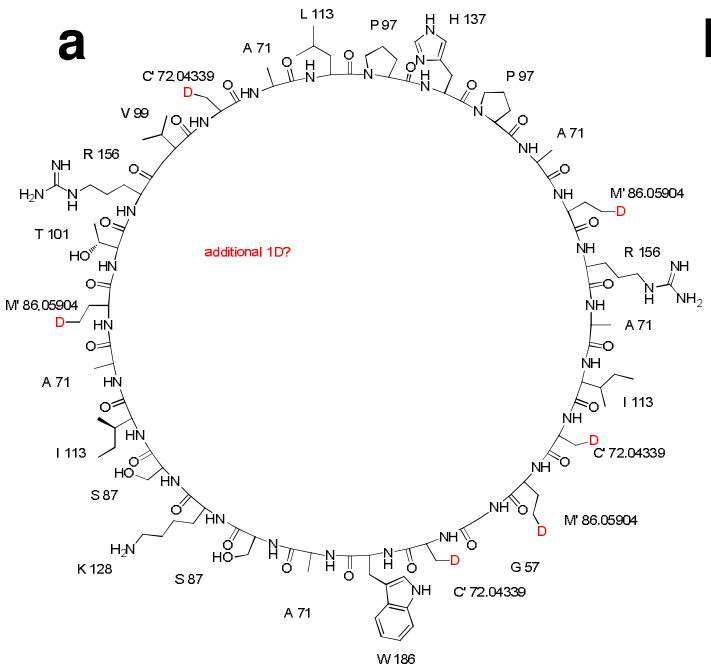
a
L 113
P 97
H 137
A 71
C' 72.04339
P 97
V 99
A 71
R 156
M' 86.05904
T 101
additional 1D?
R 156
M' 86.05904
A 71
A 71
I 113
I 113
C' 72.04339
S 87
M' 86.05904
K 128
S 87
G 57
C' 72.04339
A 71
W 186

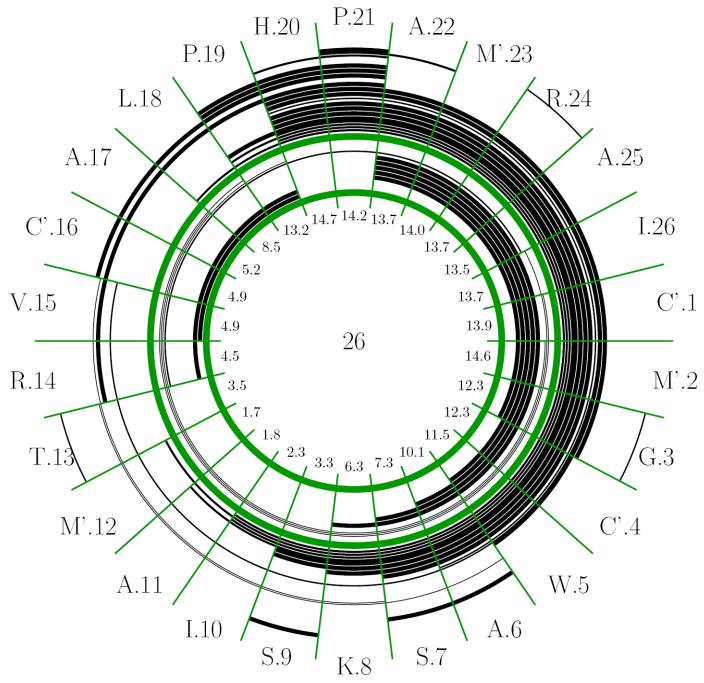
b
H.20
P.21
A.22
P.19
M'.23
L.18
R.24
A.17
A.25
C'.16
I.26
V.15
C'.1
R.14
M'.2
T.13
G.3
M'.12
C'.4
A.11
W.5
I.10
A.6
S.9
K.8
S.7
26

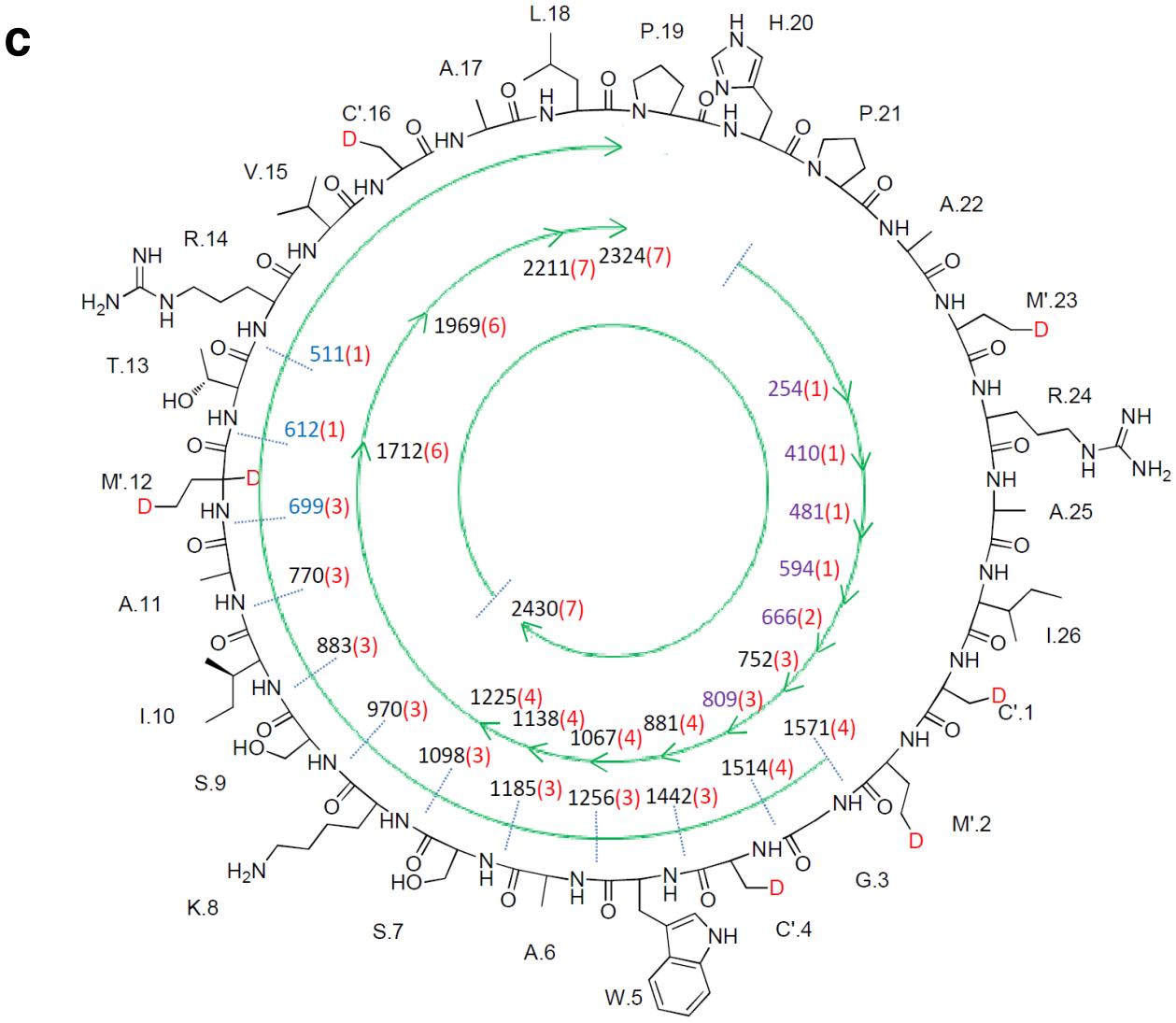
c
L.18
P.19
H.20
A.17
C'.16
P.21
V.15
A.22
R.14
M'.23
T.13
R.24
M'.12
A.25
A.11
I.26
I.10
C'.1
S.9
M'.2
K.8
G.3
S.7
C'.4
A.6
W.5
2211(7)
2324(7)
1969(6)
511(1)
254(1)
612(1)
1712(6)
410(1)
699(3)
481(1)
770(3)
2430(7)
594(1)
883(3)
666(2)
752(3)
1225(4)
809(3)
970(3)
1138(4)
881(4)
1067(4)
1571(4)
1098(3)
1514(4)
1185(3)
1256(3)
1442(3)

Supplementary Fig. 11. Comparative dereplication of SKF. a) SKF template used for comparative dereplication. Under $NaBD_4/NiCl_2$ dethiolation reaction, seven deuteriums were obtained. Six deuteriums can be predicted to be introduced from the replacement of three methionine and three cysteine side chains (red color labeled), whereas the remaining deuterium is introduced at the site of the thioether linkage. This template and the dethiolated SKF MS/MS spectrum were subjected to NPR-dereplication algorithm to compute for correlation. The least correlated residue indicates the location of the extra deuterium which allows to infer the location of thioether linkage. **b)** Comparative dereplication suggested thioether linkage on Met^{12}. Each semicircle represents an annotated peak in the MS spectrum. Peaks with multiple annotations split their count equally among the repeats. Inner numbers are the count/score of the supporting peaks for the conservation of the given amino acid. Amino acid codes have an extra index number to disambiguate repeated amino acids by their position. $Methionine^{12}$ has the lowest score indicating it bears the extra deuterium. **c**) Summary of fragments observed by CID fragmentation of deuterated dethiolated SKF. Incorporated deuteriums were labeled on structure with D (in red). Each number labeled inner the chemical structure is the mass of observed fragment with semi-circle representing the sequence. Associated number in parenthesis represents the number of deuterium within certain fragment. Each residue was labeled with one letter amino acid code as well as corresponding masses showed outside the chemical structure. Ions observed in MS^2 were showed in black color. Further supporting ions observed from MS^3 spectrum of ion *m/z* 883 were shown in blue and ions observed from MS^3 spectrum of ion *m/z* 881 were shown in purple. The corresponding ion tables are showed in **Supplementary Tables 5** and **6.**

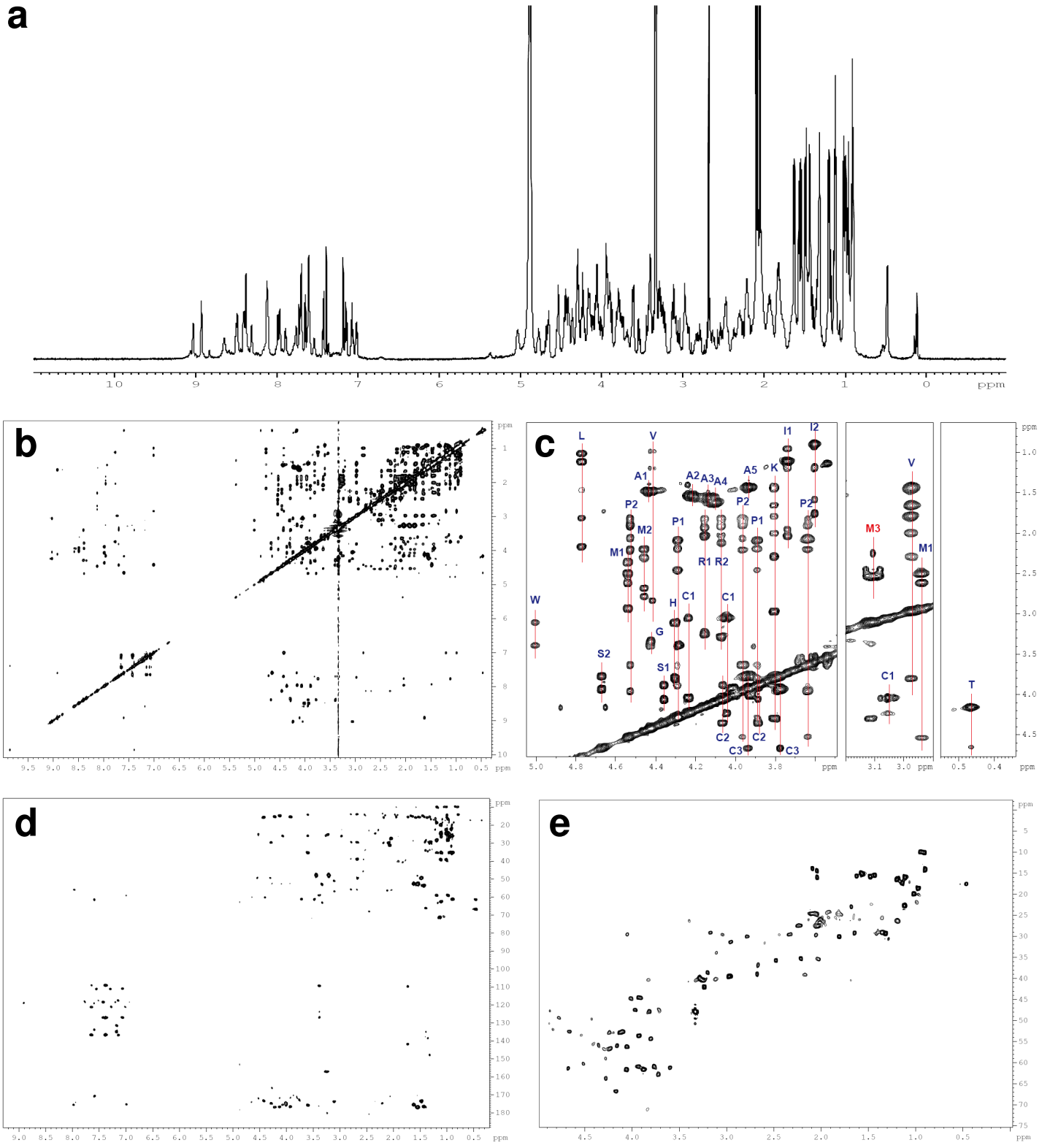

Supplementary Fig. 12. NMR spectra of SKF. a) ^{1}H NMR spectrum of SKF. The spectrum was observed in CD_3OD, 600 MHz. The detailed annotations were listed in **Supplementary Table 6**. **b, c**) ^{1}H-^{1}H TOCSY spectra and annotations of SKF. The spectrum was observed in CD_3OD, 600 MHz, with mixing time = 90 ms. subfigure b is a full spectrum whereas subfigure c is a zoom in spectrum as well as annotations. **d**) ^{1}H-^{13}C

HMBC spectrum of SKF. The spectrum was observed in CD_3OD, 600 MHz, with $^{2,3}J_{1H/13C}$ = 7 Hz. Full ^{1}H-^{13}C HMBC spectrum is shown. The annotations for critical signals supporting modified methionine are displayed in Fig 2e. **e**) ^{1}H-^{13}C HSQC spectrum of SKF. The spectrum was observed in CD_3OD, 600 MHz, with $^{1}J_{1H/13C}$ = 145 Hz. ^{1}H-^{13}C HSQC spectrum was collected to assist in HMBC spectrum annotation.

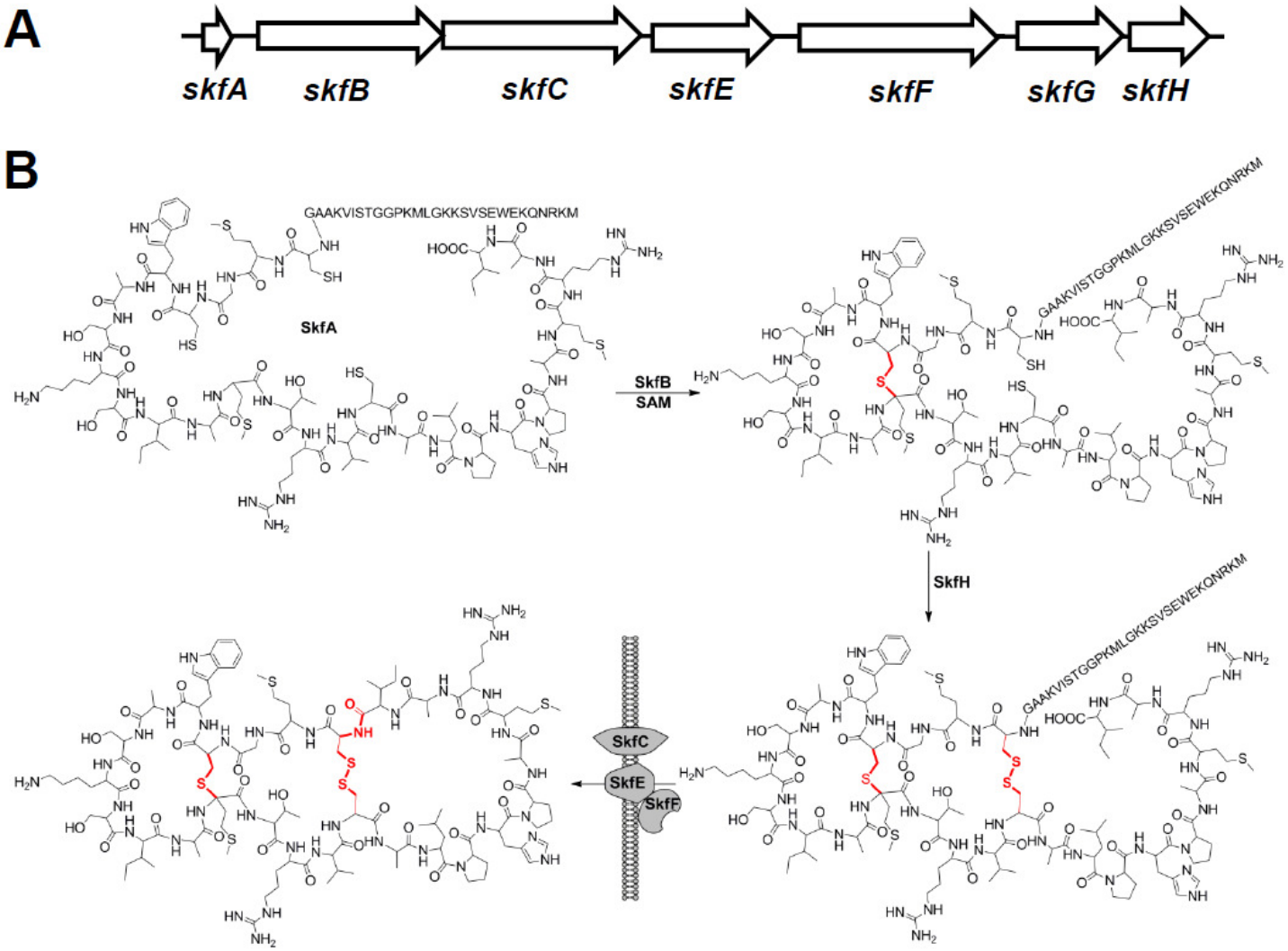

Supplementary Fig. 13. The functional annotation of the *skf* operon. (**a**) The *skf* operon. (**b**) The proposed biosynthetic pathway of SKF.

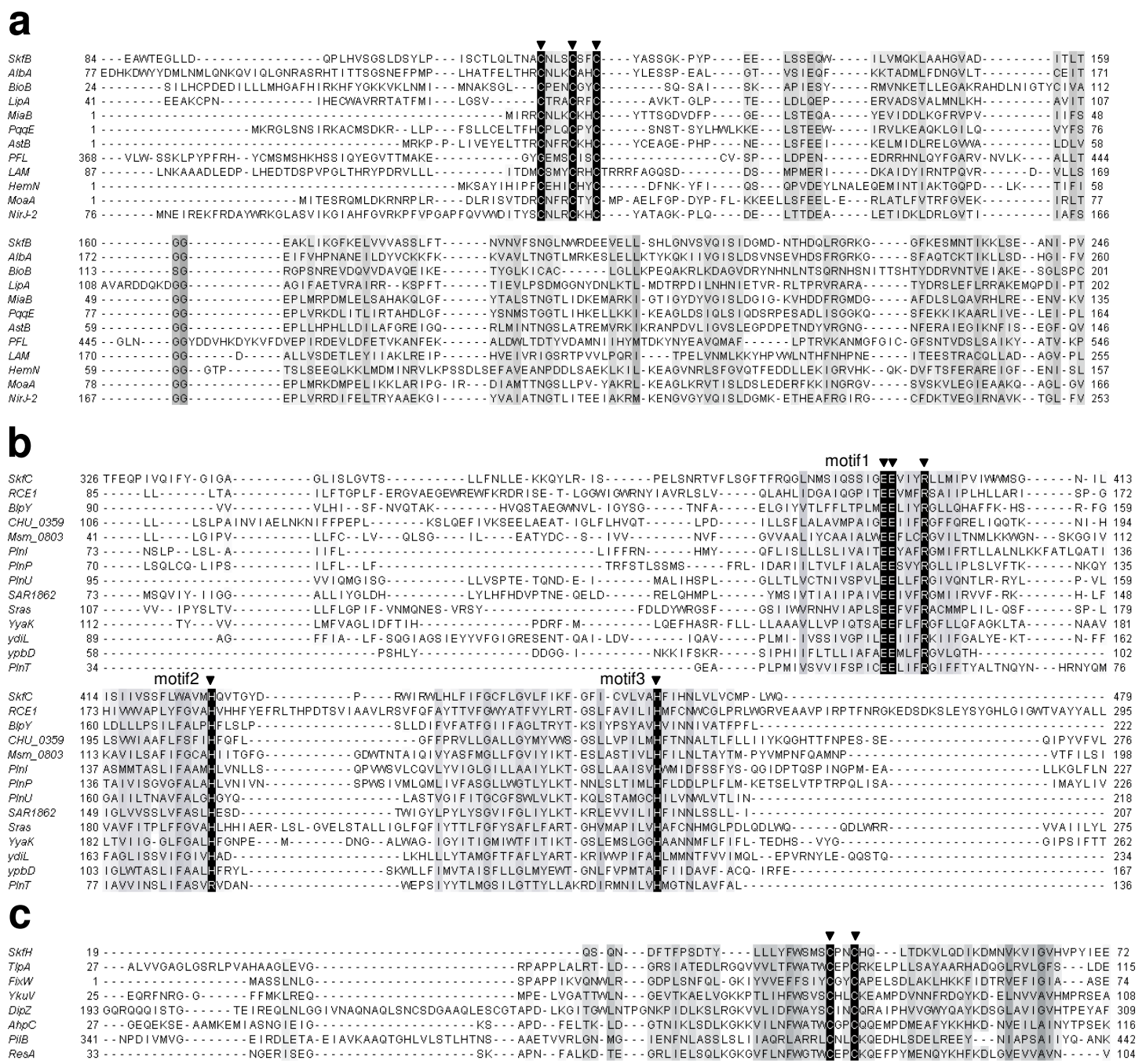

Supplementary Fig. 14. Multiple sequence alignment of SkfB, SkfC, and SkfH. a) Multiple sequence alignment of SkfB. SkfB belongs to radical SAM superfamily, along with some well-known proteins such as LAM, PFL, BioB, LipA. All members of this family show a conserved motif of CXXXCXXC (marked by ▼) which act to coordinate the iron in [4Fe-4S] cluster. **b**) Multiple sequence alignment of SkfC. Three conserved motifs are showed. The first motif contains two adjacent glutamic acid usually follows by a highly conserved

arginine spaced by three resides. The first Glu in motif1 as well as the two histidines are thought to involve in zinc binding whereas the second Glu is responsible for catalytic activity. **c**) Multiple sequence alignment of SkfH. SkfH homologs to thioredoxin showed a characteristic CXXC motif. Only the highly conserved regions are displayed due to the length variation of each protein. Alignment was done by kalign (22) using default settings. Only the highly conserved regions are displayed due to the length variation of each protein.

D. Supplementary Tables

Supplementary Table 1. Annotation of ion *m/z* 4312.6 intact cell MALDI TOF/TOF MS spectra.

Seq.	Ion	Calc. mass	Obs. Ion	Obs. Mass	Error (Da)	Seq.	Ion	Calc. mass	Obs. Ion	Obs. Mass	Error (Da)
C*	y42	4311.2111				**A**	y21	2228.1841	2229.0198	2228.0125	0.17
G	y41	4210.2176				**L**	y20	2157.1470	2158.7219	2157.7146	0.57
L	y40	4153.1961				**Q**	y19	2044.0629	2045.7079	2044.7006	0.64
Y	y39	4040.1121				**T**	y18	1916.0043	1916.7095	1915.7022	0.30
A	y38	3877.0487				**A**	y17	1814.9567	1815.6859	1814.6786	0.28
V	y37	3806.0116				**A**	y16	1743.9195	1745.5134	1744.5061	0.59
C*	y36	3706.9432				**A**	y15	1672.8824	1673.5553	1672.5480	0.33
V	y35	3603.9340	3605.5808	3604.5735	0.64	**V**	y14	1601.8453	1602.4382	1601.4309	0.41
A	y34	3504.8656	3506.2117	3505.2044	0.34	**T**	y13	1502.7769	1503.3473	1502.3400	0.44
A	y33	3433.8285	3435.6174	3434.6101	0.78	**T**	y12	1401.7292	1403.2509	1402.2436	0.51
G	y32	3362.7914	3365.7439	3364.7366	1.95	**A**	y11	1300.6816	1302.3075	1301.3002	0.62
Y	y31	3305.7699	3307.0168	3306.0095	0.24	**V**	y10	1229.6444	1231.4102	1230.4029	0.76
L	y30	3142.7066	3143.8500	3142.8427	0.14	**W**	y9	1130.5760	1131.1478	1130.1405	-0.44
Y	y29	3029.6226	3032.2168	3031.2095	1.59	**K**	y8	944.4967	946.0443	945.0370	0.54
V	y28	2866.5592	2867.4478	2866.4405	0.12	**V**	y7	816.4018			
V	y27	2767.4908	2768.2283	2767.2210	0.27	**Y**	y6	653.3384			
G	y26	2668.4224	2669.2111	2668.2038	0.22	**A**	y5	554.2700			
V	y25	2611.4009	2613.3098	2612.3025	0.90	**K**	y4	483.2329			
N	y24	2512.3325	2514.1226	2513.1153	0.78	**Y**	y3	355.1380			
A	y23	2398.2896	2399.9397	2398.9324	0.64	**S**	y2	192.0746			
V	y22	2327.2525	2328.8513	2327.8440	0.59	**S**	y1	105.0426			

Supplementary Table 2. Sytox Green cell permeability over time of SDP treatment.

Average Percent Permeabilized Cells[1] ±SD[2] (# of cells scored in each experiment)				
Timepoint	**3610[3]**	**ALB1035[3]**	**PY79**	**KP648**
30 min DMSO	1.9% (313)	0% (111)	0.6% (353)	0.3% (292)
60 min DMSO	1.1% (379)	0.7% (153)	0.8%±0.3% (186,313,318,260)	1.1%±0.1% (284,437)
90 min DMSO	2.7% (331)	0.3% (337)	0.5%±0.5% (247,320,326,435)	0.6%±0.4% (326,350)
120 min DMSO	0.3% (290)	0% (265)	0.5%±0.5 (166,329,365,321)	1.2%±1.6% (225,300)
30 min SDP	10.3% (339)	1.3% (156)	0.6% (174)	2.4% (252)
60 min SDP	4.7% (342)	7.5% (308)	4.2%±2.9% (224,250,313,215)	3.5%±1.5% (309,367)
90 min SDP	28.0% (336)	16.3% (1295)	7.5%±2.2% (271,375,290,304)	13.6%±15.1% (274,305)
120 min SDP	32.8% (344)	34.3% (507)	13.7%±1.5% (134,248,203,307)	19.8%±5.8% (301,255)

[1]The percentage of permeabilized cells for individual experiments were calculated and then averaged to generate the average percent permeabilized cells. Cell debris was not scored unless it clearly was derived from a single cell. Membrane spheres and tubules were not counted as cells.

[2]The standard deviation was calculated based on the percent permeabilized cells in repeated experiments

[3]Experiments on these strains were performed once, so no standard deviation is available

Supplementary Table 3. Membrane staining irregularities in strain 3610 after 120 minutes of SDP treatment.

Cell type	**% cells (# scored)**
Intact cells[1]	64% (314)
Irregular membrane	29% (140)
Clear gaps in membrane	7% (36)
Tubules	5% (27)[2]
Spheres	5% (26)[2]

[1]Includes permeabilized cells that had no obvious membrane deformation.

[2]Membrane tubules and spheres are subcellular particles, so the scoring indicates the frequency with which such structures were observed relative to the total number of cells scored.

Supplementary Table 4. Annotations of SDP FT MS/MS spectrum. Errors are in ppm.

Seq.	Ion	Calc. mass	Obs. ion	Obs. mass	Error	Ion	Calc. mass	Obs. ion	Obs. mass	Error
C*	b1	103.0092				y42	4311.2111			
G	b2	160.0307				y41	4210.2176			
L	b3	273.1147				y40	4153.1961			
Y	b4	436.1780				y39	4040.1121			
A	b5	507.2152				y38	3877.0487			
V	b6	606.2836				y37	3806.0116			
C*	b7	707.2771	708.2770	707.2697	10.42	y36	3706.9432			
V	b8	806.3455	807.3433	806.3360	11.76	y35	3603.9340	1802.9338	3603.8530	22.47
A	b9	877.3826	878.3798	877.3725	11.50	y34	3504.8656	1753.4027	3504.7908	21.34
A	b10	948.4197	949.4153	948.4080	12.34	y33	3433.8285	1717.8869	3433.7592	20.17
G	b11	1005.4412	1006.4351	1005.4278	13.29	y32	3362.7914	1682.3684	3362.7222	20.57
Y	b12	1168.5045	1169.4938	1168.4865	15.40	y31	3305.7699	1653.8592	3305.7038	20.00
L	b13	1281.5886	1282.5748	1281.5675	16.42	y30	3142.7066	1572.3325	3142.6504	17.87
Y	b14	1444.6519	1445.6347	1444.6274	16.95	y29	3029.6226	1515.7906	3029.5666	18.45
V	b15	1543.7203	1544.7019	1543.6946	16.64	y28	2866.5592			
V	b16	1642.7887	1643.7614	1642.7541	21.06	y27	2767.4908	1384.7287	2767.4428	17.33
G	b17	1699.8102	1700.7851	1699.7778	19.04	y26	2668.4224	1335.1968	2668.3790	16.25
V	b18	1798.8786	1799.8453	1798.8380	22.55	y25	2611.4009	1306.6889	2611.3632	14.44
N	b19	1912.9215	1913.8818	1912.8745	24.57	y24	2512.3325	1257.1545	2512.2944	15.16
A	b20	1983.9586				y23	2398.2896	1200.1330	2398.2514	15.91
V	b21	2083.0270				y22	2327.2525	1164.6165	2327.2184	14.63
A	b22	2154.0642				y21	2228.1841	1115.0821	2228.1496	15.46
L	b23	2267.1482				y20	2157.1470	1079.5659	2157.1172	13.78
Q	b24	2395.2068				y19	2044.0629	1023.0255	2044.0364	12.95
T	b25	2496.2545				y18	1916.0043	958.9989	1915.9832	11.01
A	b26	2567.2916				y17	1814.9567	1815.9249	1814.9176	21.50
A	b27	2638.3287				y16	1743.9195	1744.8932	1743.8859	19.28
A	b28	2709.3658				y15	1672.8824	1673.8595	1672.8522	18.06
V	b29	2808.4342				y14	1601.8453	1602.8207	1601.8134	19.91
T	b30	2909.4819				y13	1502.7769	1503.7552	1502.7479	19.29
T	b31	3010.5296				y12	1401.7292	1402.7101	1401.7028	18.84
A	b32	3081.5667				y11	1300.6816	1301.6685	1300.6612	15.63
V	b33	3180.6351				y10	1229.6444	1230.6321	1229.6248	15.96
W	b34	3366.7144				y9	1130.5760	1131.5661	1130.5588	15.22
K	b35	3494.8094				y8	944.4967	945.4916	944.4843	13.13
V	b36	3657.8727				y7	816.4018	817.3993	816.3920	11.93
Y	b37	3756.9411				y6	653.3384			
A	b38	3827.9782				y5	554.2700			
K	b39	3956.0732				y4	483.2329			
Y	b40	4119.1365				y3	355.1380			
S	b41	4206.1685				y2	192.0746			
S	b42	4293.2006				y1	105.0426			

Supplementary Table 5. Annotations of critical ions observed in deuterated dethiolated SKF MS/MS spectrum analyzed by FT-ICR MS.

Calc. Mass 1[a]	D number[b]	Calc. Mass 2[c]	Obs Mass	Error (ppm)	Annotation[d]
749.4547	3	752.4736	752.4733	-0.3	PAM'RAIC'M'
767.4654	3	770.4842	770.4802	-5.2	AM'TRVC'AL
877.5133	4	881.5384	881.5395	1.2	PAM'RAIC'M'GC'
880.5495	3	883.5683	883.5648	-3.9	IAM'TRVC'AL
967.5815	3	970.6003	970.6006	0.3	SIAM'TRVC'AL
1063.5926	4	1067.6177	1067.6171	-0.6	PAM'RAIC'M'GC'W
1095.6765	3	1098.6953	1098.6955	0.2	KSIAM'TRVC'AL
1134.6298	4	1138.6548	1138.6530	-1.6	PAM'RAIC'M'GC'WA
1182.7085	3	1185.7273	1185.7267	-0.5	SKSIAM'TRVC'AL
1221.6618	4	1225.6869	1225.6763	-8.6	PAM'RAIC'M'GC'WAS
1253.7456	3	1256.7644	1256.7656	1.0	ASKSIAM'TRVC'AL
1439.8249	3	1442.8438	1442.8402	-2.4	WASKSIAM'TRVC'AL
1510.8621	4	1514.8871	1514.8793	-5.2	C'WASKSIAM'TRVC'AL
1567.8835	4	1571.9086	1571.8966	-7.7	GC'WASKSIAM'TRVC'AL
1705.9627	6	1712.0004	1711.9916	-5.1	PAM'RAIC'M'GC'WASKSIAM'
1963.1115	6	1969.1492	1969.1343	-7.5	PAM'RAIC'M'GC'WASKSIAM'TR
2204.2542	7	2211.2981	2211.3032	2.3	PAM'RAIC'M'GC'WASKSIAM'TRVC'A
2317.3384	7	2324.3822	2324.3689	-5.7	PAM'RAIC'M'GC'WASKSIAM'TRVC'AL
2423.3550	7	2430.3989	2430.3984	-0.2	SIAM'TRVC'ALPHPAMRAIC'M'GC'WAS

a. Theoretical mass of fragment ions resulted from $NaBH_4$ reduction (dethiolated SKF).

b. D number represents for the number of deuterium labeled within certain fragments.

c. Theoretical mass of fragment ions resulted from $NaBD_4$ reduction (deuterated dethiolated SKF).

d. Residue C and M are marked due to the reason that these two residues are derivatized after reaction.

Supplementary Table 6. Annotations of critical ions observed in additional fragmentation (MS3) of deuterated dethiolated SKF analyzed by IT-MS.

Calc. Mass 1[a]	D number[b]	Calc. Mass 2[c]	Obs Mass	Error (Da)	Annotation[d]
510.33	1	511.33	511.26	-0.07	RVC'AL
611.38	1	612.38	612.35	-0.03	TRVC'AL
696.43	3	699.45	699.44	0.00	M'TRVC'AL
806.48	3	809.50	809.44	-0.05	PAM'RAIC'M'G
664.40	2	666.41	666.44	0.03	PAM'RAIC'
593.36	1	594.37	594.44	0.07	PAM'RAI
480.28	1	481.29	481.35	0.07	PAM'RA
409.24	1	410.25	410.35	0.10	PAM'R
253.14	1	254.15	253.99	-0.16	PAM’

a. Theoretical mass of fragment ions resulted from $NaBH_4$ reduction (dethiolated SKF).

b. D number represents for the number of deuterium labeled within certain fragments.

c. Theoretical mass of fragment ions resulted from $NaBD_4$ reduction (deuterated dethiolated SKF).

d. Residue C and M are marked due to the reason that these two residues are derivatized after reaction.

Supplementary Table 7. ^{1}H NMR data of SKF.

	NH	α	β	γ	others
A1	7.93	4.43	1.48		
A2	7.98	4.22	1.54		
A3	8.11	4.13	1.56		
A4	8.91	4.1	1.62		
A5	8.40	3.93	1.43		
C1	9.02	4.23	3.05, 4.04		
C2	7.98	4.35	3.88, 4.06		
C3	8.38	4.67	3.78, 3.93		
G	8.39	3.39, 4.28			
H	8.03	5.00	3.10, 3.40		8.58 (NH), 7.18
I1	7.60	3.74	2.04	1.11 (CH_3), 1.19, 1.96	1.01 (δ)
I2	8.47	3.6	1.76	0.89 (CH_3), 1.19, 1.59	0.91 (δ)
K	7.73	4.28	2.29	1.79, 1.99	1.43 (δ), 1.65 (δ), 2.97 (ε)
L	7.60	4.77	1.46, 2.17	1.81	1.01 (δ), 1.12 (δ)
M1	7.52	4.54	2.36, 2.51	2.62, 2.94	2.09 (SCH_3)
M2	8.13	4.46	2.20, 2.31	2.69, 2.79	2.07 (SCH_3)
M3	ND	-	2.25, 2.46	2.54, 3.10	2.04 (SCH_3)
P1	-	4.29	2.09, 2.46	2.09, 2.19	3.65 (δ), 3.90 (δ)
P2	-	4.53	1.91, 2.21	1.81, 2.07	3.64 (δ), 3.97 (δ)
R1	7.96	4.15	2.03	1.83, 1.94	7.44 (NH), 3.25 (δ)
R2	7.98	4.07	2.10	1.82, 1.92	7.53 (NH), 3.28 (δ)
S1	7.99	4.36	3.88, 4.07		
S2	8.38	4.67	3.77, 3.93		
T	7.59	4.65	4.16	0.47	
V	7.77	4.42	2.84	0.98, 1.20	
W	8.34	4.30	3.11, 3.80		9.85 (NH), 7.39 (s), 7.66 (d), 7.07 (t), 7.15 (t), 7.43 (d)

D. References

S1. Gonzalez-Pastor JE, Hobbs EC, Losick R (2003) Cannibalism by sporulating bacteria. *Science* 301:510–513.

S2. Ngoka LCM, Gross ML (1999) Multistep tandem mass spectrometry for sequencing cyclic peptides in an ion-trap mass spectrometer. *J Am Soc Mass Spectrom* 10:732–746.

S3. Kawulka KE, et al. (2004) Structure of subtilosin A, a cyclic antimicrobial peptide from *Bacillus subtilis* with unusual sulfur to alpha-carbon crosslinks: Formation and reduction of alpha-thio-alpha-amino acid derivatives. *Biochemistry* 43:3385–3395.

S4. Ng J, et al. (2009) Dereplication and *de novo* sequencing of nonribosomal peptides. *Nat Methods* 6:596–599.

S5. Oman TJ, van der Donk WA (2010) Follow the leader: the use of leader peptides to guide natural product biosynthesis. *Nat Chem Biol* 6:9–18.

S6. Miller JR, et al. (2000) *Escherichia coli* LipA is a lipoyl synthase: *In Vitro* biosynthesis of lipoylated pyruvate dehydrogenase complex from octanoyl-acyl carrier protein. *Biochemistry* 39:15166–15178.

S7. Sofia HJ, Chen G, Hetzler BG, Reyes-Spindola JF, Miller NE (2001) Radical SAM, a novel protein superfamily linking unresolved steps in familiar biosynthetic pathways with radical mechanisms: functional characterization using new analysis and information visualization methods. *Nucl Acids Res* 29:1097–1106.

S8. Berkovitch F, Nicolet Y, Wan JT, Jarrett JT, Drennan CL (2004) Crystal structure of biotin synthase, an S-adenosylmethionine-dependent radical enzyme. *Science* 303:76–79.

S9. McIntosh JA, Donia MS, Schmidt EW (2009) Ribosomal peptide natural products: bridging the ribosomal and nonribosomal worlds. *Nat Prod Rep* 26:537–559.

S10. Pei J, Grishin NV (2001) Type II CAAX prenyl endopeptidases belong to a novel superfamily of putative membrane-bound metalloproteases. *Trends Biochem Sci* 26:275–277.

S11. Dorenbos R, et al. (2002) Thiol-disulfide oxidoreductases are essential for the production of the lantibiotic sublancin 168. *J Biol Chem* 277:16682–16688.

S12. Branda SS, Gonzalez-Pastor JE, Ben-Yehuda S, Losick R, Kolter R (2001) Fruiting body formation by *Bacillus subtilis*. *Proc Natl Acad Sci* USA 98:11621–11626.

S13. Youngman P, Perkins JB, Losick R (1984) Construction of a cloning site near one end of Tn917 into which foreign DNA may be inserted without affecting transposition in Bacillus subtilis or expression of the transposon-borne erm gene. *Plasmid* 12:1–9.

S14. Pogliano J, Sharp M, Pogliano K (2002) Chromosome partitioning during establishment of cellular asymmetry in *Bacillus subtilis*. *J Bact* 184:1743–1749.

S15. Ireton K, Rudner DZ, Siranosian KJ, Grossman AD (1993) Integration of multiple developmental signals in Bacillus subtilis through the Spo0A transcription factor. *Genes Dev* 7:283–294.

S16. Ellermeier CD, Hobbs EC, Gonzalez-Pastor JE, Losick RA (2006) Three-Protein Signaling Pathway Governing Immunity to a Bacterial Cannibalism Toxin. *Cell* 124:549–559.

S17. Yang YL, Xu Y, Straight P, Dorrestein PC (2009) Translating metabolic exchange with imaging mass spectrometry. *Nat Chem Biol* 5:885–887.

S18. Puolitaival SM, Burnum KE, Cornett DS, Caprioli RM (2008) Solvent-free matrix dry-coating for MALDI imaging of phospholipids. *J Am Soc Mass Spectrom* 19:882–886.

S19. Becker EC, Pogliano K (2007) Cell-specific SpoIIIE assembly and DNA translocation polarity are dictated by chromosome orientation. *Mol Microbiol* 66:1066–1079.

S20. Leenders F, Stein TH, Kablitz B, Franke P, Vater J (1999) Rapid Typing of Bacillus subtilis Strains by their Secondary Metabolites Using Matrix-Assisted Laser Desorption/Ionization Mass Spectrometry of Intact Cells *Rapid Commun Mass Spectrom* 13:943–949.

S21. Erhard M, von Döhren H, Jungblut P (1997) Rapid typing and elucidation of new secondary metabolites of intact cyanobacteria using MALDI-TOF mass spectrometry. *Nat Biotechnol* 15:906–909.

S22. Lassmann T, Sonnhammer ELL (2006) Kalign, Kalignvu and Mumsa: web servers for multiple sequence alignment. *Nucl Acids Res* 34:596–599.